# (e,2e) spectrometer for investigating the spectral momentum density of thin films

A. L. Ritter, J. R. Dennison, and J. Dunn

# (e, 2e) spectrometer for investigating the spectral momentum density of thin films

A. L. Ritter, J. R. Dennison, and J. Dunn

*Department of Physics, Virginia Polytechnic Institute and State University, Blacksburg, Virginia 24061*

An (e, 2e) spectrometer has been constructed for detecting scattered and recoiling electrons from a thin solid film. The cross section for observing the two electrons in coincidence is proportional to the spectral momentum density of the target. In this spectrometer the energy of the incident electron beam is 25 keV and the beam current is approximately 40 $\mu$A. The energy resolution (FWHM) is $\leqslant 4$ eV. The momentum resolution (FWHM) can be varied from 0.2 to 1.0 Å$^{-1}$. Preliminary coincidence data from an amorphous carbon film are presented.

This is a preliminary report on the construction of a new electron scattering spectrometer for observing scattered and recoiling electrons in coincidence, a technique now referred to as (e, 2e) spectroscopy. The first (e, 2e) experiments on thin carbon films were done approximately 15 years ago.[1,2] Subsequent experiments[3,4] predominantly investigated the electronic structure of atoms and molecules in gaseous targets because severe technical difficulties were encountered in applying the technique to thin foils. This paper describes an (e, 2e) spectrometer for investigating films which is designed to mitigate these problems to a significant degree.

The mechanics of (e, 2e) scattering is conceptually straightforward. A high-energy electron ($E_0$ = several keV) incident on the sample scatters from an electron in the target. Those events in which the scattered and recoiling electrons leave the target with equal energy (and, therefore, close to 45° with respect to the incident beam) are detected by coincidence techniques. The precollision energy $E_b = E_s + E_r - E_0$ and momentum $\mathbf{q} = \mathbf{P}_s + \mathbf{P}_r - \mathbf{P}_0$ of the target electron can be determined from the energy and momenta of the two scattered electrons $E_s, \mathbf{P}_s$ and $E_r, \mathbf{P}_r$ (in deriving the expression for $E_b$ and $\mathbf{q}$ it was assumed that the target had infinite mass). Generally, $E_s$ and $E_r$ are chosen equal so that both electrons leave the target with high energy and, therefore, have a low probability of multiple scattering. A schematic of the process is shown in Fig. 1.

The unique feature of (e, 2e) scattering is that under general conditions which are satisfied well in our spectrometer the cross section is proportional to the spectral momentum density $p(E, \mathbf{q})$ [ $p(E, \mathbf{q}) \, dE \, d\mathbf{q}$ is the probability of finding an electron in the system with energy $E$ and momentum $\mathbf{q}$]. This fundamental quantity is equal in the independent electron approximation to the momentum density of those occupied electron states in the energy interval $E$ to $E + dE$. In a series of detailed experiments on simple atomic systems, such as atomic hydrogen[5] and helium,[6–8] the theoretical and measured cross sections were in perfect agreement, within experimental error, over a wide range of experimental parameters. Most of the approximations made in analyzing data from atomic systems are also applied to the analysis of data from thin solid films. The notable agreement between

theory and experiment for hydrogen and helium is strong support for the basic theoretical assumptions necessary for extracting the spectral momentum density from the measured cross section.

There have been two general approaches to the design of (e, 2e) spectrometers for gaseous targets. The first spectrometers consisted of an electron gun and two detectors which could be moved mechanically to different scattering angles. Data were taken in serial order for each ($E, q$) value of interest. A second approach taken by Moore et al.[9] is a multidetector system which allows parallel collection of data at 25 scattering angles. In both these approaches the incident energy is less than or of the order of a few thousand electron volts. In order to study thin films, the incident energy must be at least an order of magnitude higher to minimize multiple scattering sufficiently.

The incident energy for our spectrometer is 25 keV. The mean free path for a typical material is then a few hundred angstroms. This is about the minimum thickness for a self-supporting film. This necessarily high incident energy, in turn, drastically reduces the count rate which goes as $E_0^{-2.5}$ (assuming the film thickness is scaled with $E_0$). If the incident beam current is kept the same for gas and thin films (10 to 100 $\mu$A), then the count rate would be comparable in the two cases. The higher density of solid targets relative to the den-



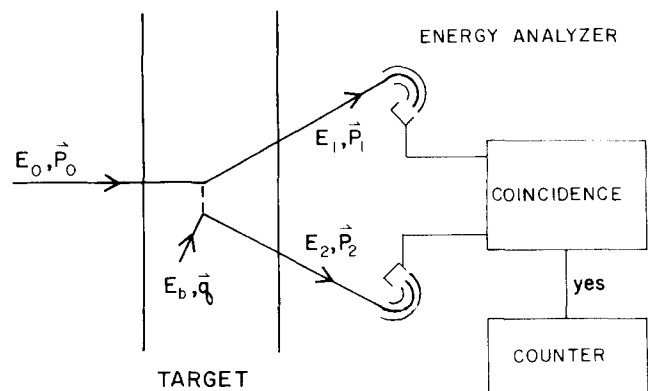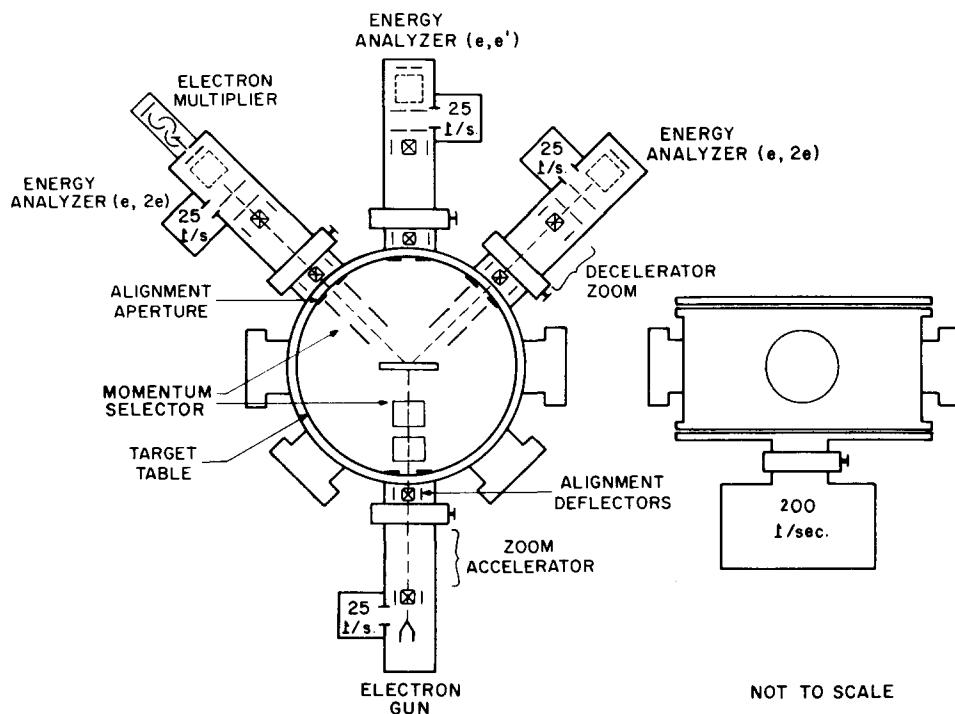FIG. 1. Schematic representation of (e, 2e) scattering.

© 1984 American Institute of Physics    1280

FIG. 2. Schematic of the (e, 2e) spectrometer.

sity of gas targets compensates for the energy dependence of the cross section. In the initial experiments on thin films, the beam current was limited to 0.1 $\mu$A because of target damage. In order to maintain a reasonable count rate (typically 0.01 to 1 Hz), the energy resolution was degraded to 100 eV. The valence-band structure, of course, could not be resolved in these experiments. The target damage apparently was due to the relatively poor vacuum ($10^{-7}$ to $10^{-6}$ Torr) in these first investigations. We use mag-ion pumps in our system and take data with pressures in the mid to upper $10^{-9}$-Torr range. We have taken data continuously on a carbon film for over 1 month with beam currents of approximately 40 $\mu$A.

In addition to the problem of target damage, the high incident beam energy also places stringent requirements on measuring accurately the scattering angles. Determination of the momentum with a precision $\Delta q_{FWHM} = 0.2$ Å$^{-1}$ requires that the scattering angle be measured to better than 3 mrad. It would be prohibitively difficult to move the detectors mechanically and keep this precision. We employ electrostatic deflectors positioned accurately on a 27.9-cm-diam stainless-steel table to vary the scattering angle.

A schematic of the spectrometer is shown in Fig. 2. The scattering chamber and beam-arm vacuum jackets are constructed of stainless steel. A 200-I/s mag-ion pump on the target chamber and 25-I/s mag-ion pumps on each beam arm provide a base pressure of $3 \times 10^{-9}$ Torr. The chamber and beam arms can be isolated by gate valves so that samples can be changed without cycling the electron gun and electron multipliers to atmosphere each time. The target chamber and beam lines are electrically isolated by beam line insulators made by National Electrostatics Corporation. The electron gun (Cliftronic 3K/5U) provides 10 to 100 $\mu$A of current at 1-kV anode potential. After leaving the e gun, the beam passes through a constant-focus variable-magnification "zoom" lens. The angular divergence of the beam on

the target (which is directly proportional to the momentum resolution $\Delta q$) can be varied by a factor of 5 with this lens. The count rate for (e, 2e) scattering is proportional to $\Delta q^4$ so the zoom lens gives important flexibility in balancing the conflicting requirements of high count rate and maximum momentum resolution.

Another feature of our spectrometer is that it gives us the capability to study small-angle inelastic electron scattering using an output beam arm which is collinear with the input beam. A sample can be characterized quickly using the forward scattered beam before attempting the more difficult and time-consuming (e, 2e) experiment.

In a typical (e, 2e) investigation of an atom or molecule, the binding energies of the different electronic levels are determined first and then the momentum density of each level is measured by varying the scattering angle. Since the energy–momentum relation for the valence bands in solids often has considerable dispersion, it is more appropriate to scan simultaneously a 2-D range of energy momentum. We use a computer to log data automatically over the entire E–q range. In order to minimize systematic errors arising from the inevitable drift in beam current and transmission efficiency, the computer sweeps many times over the range of interest.

In the next section the electron optics for our spectrometer is described in more detail. In subsequent sections further details are given for scattering angle deflectors, the dc voltage distribution, the pulse electronics, and the magnetic shielding. The last section describes preliminary measurements taken with the spectrometer.

## I. ELECTRON OPTICS

The critical factors which entered into the design of the electron optics were: (1) The maximum momentum resolution should be of order 10% of a typical Brillouin zone wave
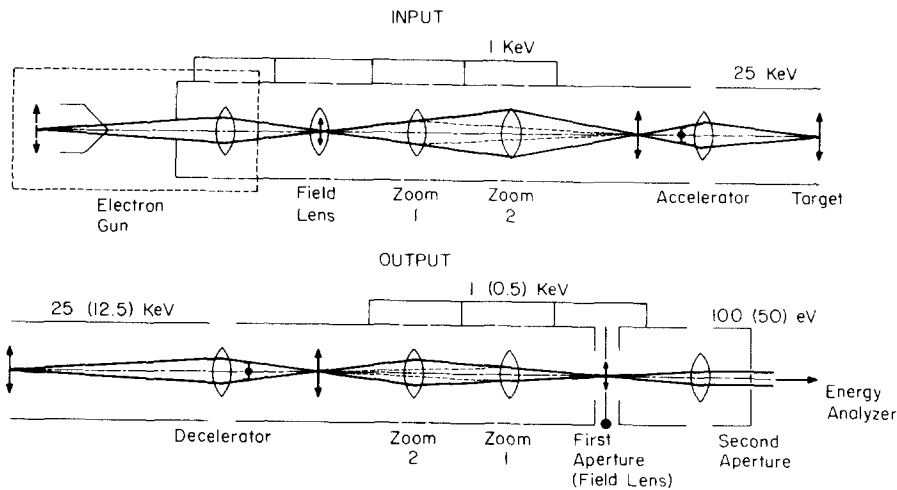
INPUT



FIG. 3. Electron optics for the input and output beams. The kinetic energy of the electron at different lens locations is indicated. The kinetic energy in parentheses on the output drawing is for the (e, 2e) beam arm. The adjacent value is for the (e, e') beam arm.

vector. We chose the momentum resolution (FWHM) to be in the range $0.2 \leqslant \Delta q \leqslant 1$ Å$^{-1}$. (2) The filling factor in the various lenses should be less than 50%. (3) In order to keep the electron gun and electron multipliers under vacuum when changing samples, there should be valves between target chamber and beam arms. The target chamber should be reasonably large (30 cm diameter in our case) in order to hold several samples and to have experimental flexibility. As a consequence of these two factors, the electron lens for controlling the input and output beam are over 30 cm from the target. (4) We chose to use a commercial electron gun (Cliftronics modified 3K/5U). (5) We chose an incident beam energy of 25 keV (incident momentum = 81 Å$^{-1}$). We estimated this energy would give us a coincidence rate $\geqslant 0.01$ Hz. (6) We chose the Wien filter (crossed $E$–$B$ fields) for the energy analyzer. The dispersion factor for the Wien filter is not as good as for other analyzers, but we were seeking modest energy resolution and limited angular acceptance. Therefore, the simplicity of the Wien filter and its straight-through geometry were overriding considerations.

The final optics design was determined by the emittance of the e gun, the desired momentum resolution, and the acceptance of the energy analyzer.

The emittance of our electron gun is approximately 0.2 cm mrad at a beam energy of 1000 eV. The Helmholtz–Lagrange constant, (emittance) times (kinetic energy)$^{1/2}$, is conserved in an electron optics system if there is no sink or source of current and if there are no energy-dispersing devices. This constant and the chosen momentum resolution constrain the electron optics for the incident and scattered beam. The total momentum resolution (FWHM) is $\Delta q^2 = P_0^2 (\theta_i^2 + \theta_0^2)$, where $P_0$ is the momentum of the incident beam, $\theta_i$ is the pencil angle of the incident beam on the target, and $\theta_0$ is the pencil angle of the scattered beam defined by the acceptance apertures. The electron optics are designed such that the beam angles for the incident and scattered beam are zero (see Kuyatt[10] for the definition of pencil and beam angle). The chosen momentum resolution is one constraint on $\theta_i$ and $\theta_0$. In order to determine the two angles, we assume the diameter of the scattered beam at the target is a factor $1/\sqrt{2}$ smaller than the incident beam diameter. We also chose the Helmholtz–Lagrange constant for the scat-

tered and incident beam to be equal. This implies $\theta_0 = 2^* \theta_i$ and $0.0011 \leqslant \theta_i \leqslant 0.0055$. These values of the pencil angle at the target and the Helmholtz–Lagrange constant govern the electron optics of the input and output beam arms.

Starting with the input beam, the electron gun is a space-charge-limited diode. Assuming the anode hole of the gun is the initial beam window, then the pupil is a virtual image approximately $3D$ ($D$ is the spacing between the cathode and anode) behind the anode. An einzel lens in the gun focuses this pupil to the center of a field lens. The first image of the window is close to infinity. The pupil and window images are input to a variable-magnification constant-focus zoom lens. The pupil image in the field lens is focused by the zoom lens to an intermediate image which, in turn, is projected by the accelerator (1 to 25 keV) onto the target. The field lens is adjusted so that the window is focused by the zoom lens to the focal point of the accelerator. The final image of the window is then projected to infinity.

Mechanical considerations dictated that the focal planes of the accelerator be over 30 cm from the target. In order to minimize the total length of the beam arm and the electron beam filling factors in the various lenses, we chose the angular magnification of the accelerator to be 0.065 and the angular magnification of the zoom to be variable, $1.65 < m < 8.25$.

The acceptance phase space for the scattered beam in both the (e, e') and (e, 2e) beam arms is defined by two apertures just before the energy analyzer. The optics in the (e, e') beam arms for the decelerator and output zoom are a mirror image of the incident beam optics. In the (e, 2e) beam arms, the kinetic energy of the detected electrons is half the energy of the incident beam (minus half the binding energy of the target electron, which energy is negligible). The geometries of the (e, 2e) and (e, e') lenses are identical, but the voltages on the (e, 2e) elements are half the respective voltages on the (e, e') lens. Since the voltage ratios are the same in both cases, the electron optics for the (e, e') and (e, 2e) beams are identical.

In both the (e, e') and (e, 2e) modes, the beam spot on the target is imaged into the first aperture by the decelerator and zoom. The second aperture defines the accepted solid angle for electrons leaving the target. The output window which is
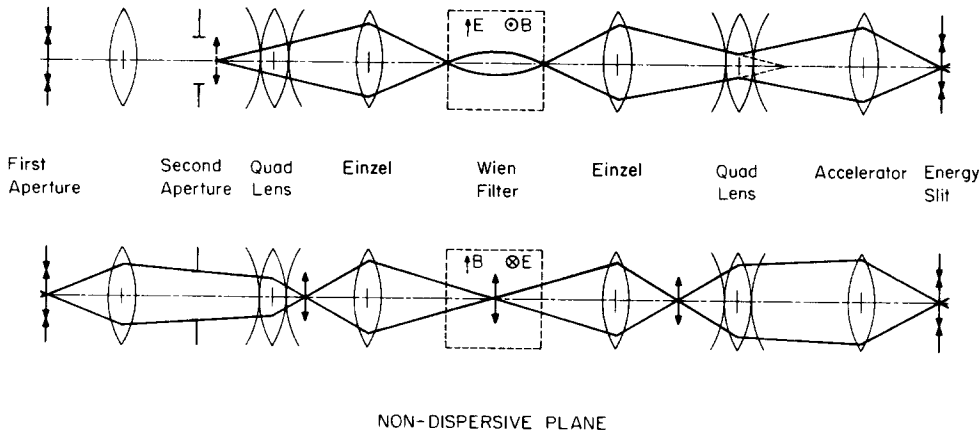
(e, 2e) spectrometer

First Aperture    Second Aperture    Quad Lens    Einzel    Wien Filter    Einzel    Quad Lens    Accelerator    Energy Slit

FIG. 4. Electron optics for the energy analyzer in two orthogonal planes.

NON-DISPERSIVE PLANE

focused into this aperture is initially at infinity. The first aperture is also a field lens which gives us the necessary degree of freedom to focus the window into the second aperture. The filling factor in the field lens is approximately 1, which generally is a bad design for electron optics because of the resulting aberrations. We decided to take this unorthodox approach because (1) there is an image in the first aperture which reduces the aberration associated with large filling factors, (2) it is possible to obtain short focal lengths with quite low voltages between the elements of the aperture lens because of the small diameter of the lens, and (3) the total number of lenses was reduced considerably by this approach. We did not observe significant effects of excessive aberration using this technique.

The first and second aperture provide the input for the energy analyzer. The Wien filter can be operated in several modes. The mode shown in Fig. 4 gives the highest energy dispersion. The electric field in the Wien filter is produced by two plates which are $2.54 \times 2.54$ cm square and are 0.508 cm apart. The magnetic field is created by two pairs of coils wrapped on the surface of a cylindrical form. The axis of the coils, of course, is perpendicular to the beam and the electric field. The placement of the coils which maximizes the homogeneity of the magnetic field is described by Anderson.[11] A mu-metal shield fits closely around the Wien filter. The analyzer was designed to have an energy resolution of 0.5 eV (FWHM). The measured width of the elastic peak was 2 to 4 eV (FWHM) at a beam current of 40 $\mu$A.

## II. SCATTERING ANGLE DEFLECTORS

As shown in Fig. 2, the input, $(e, e')$ and $(e, 2e)$ beam lines are in a plane with the $(e, 2e)$ arms at 45° with respect to the incident beam axis. There are two pairs of deflectors in front of the target which rotate the incident beam up and down by an angle $\delta$ (see Fig. 5). Only if the target electron has momentum $q = P_0\delta$ (assuming small angle limit) perpendicular to the beam line plane will the two scattered electrons enter the apertures in the $(e, 2e)$ beam lines. The voltages on the two pairs of deflectors have the ratio $V_1/V_2 = 3$. The distance between the two pairs is twice the distance from the second pair to the target. This configuration ensures (at least

in first order) that the beam will be rotated on the target without being translated out of the beam line plane, irrespective of the deflector's length. An identical set of deflectors after the target is in each $(e, 2e)$ beam path. They allow us to detect electrons with momentum parallel to the incident beam, where momentum is

$$q = 2P_1 \cos \theta - P_0$$

$$\sim - P_0 \Delta \theta ,$$

where $\Delta \theta = \theta - 45°$. The electric fields produced by these deflectors are parallel to the beam line plane. The plates for all these deflectors are 3.05 cm square and 0.76 cm apart. The rotation angle of the beam, $\Delta \theta$ or $\delta \theta$, is related to the potential $V_2$ across the deflectors by $\delta = eV_2L/4ES$, where $E$ is the kinetic energy of the electrons, $L$ is the effective length of the deflectors, and $S$ is the separation between the plates. The rotation per volt is $\delta/V_2 = 0.088$ mrad/V and $\Delta\theta/V_2 = 0.176$ mrad/V assuming the fringe fields increase the effective length of the deflectors by 10%. The incident beam deflectors were calibrated using the $(e, e')$ mode and observing Bragg diffraction from polycrystalline aluminum films. The measured dispersion is $\delta/V_2 = 0.1$ mrad/V, in good agreement with the calculated value.
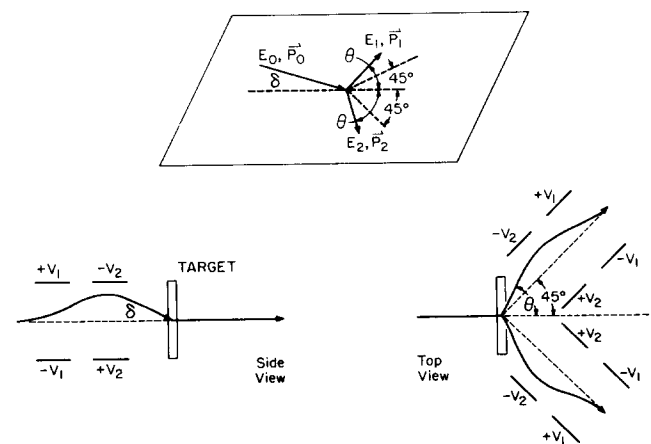


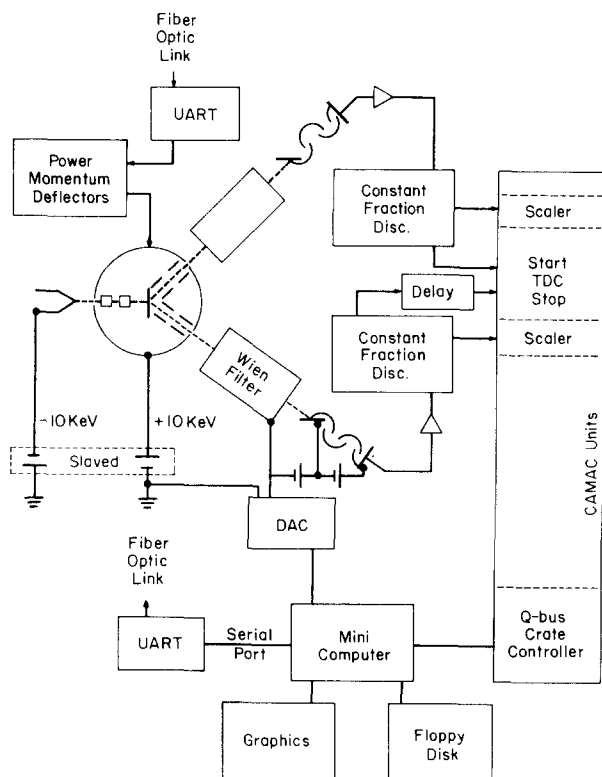FIG. 5. Electrostatic deflectors for varying the scattering geometry.

FIG. 6. Electronics for data acquisition under computer control.

It is difficult to align the input and output beam lines with the precision required for accurate determination of the scattering angles. The necessary precision is achieved by placing the target holder, scattering angle deflectors, and beam alignment apertures on a carefully machined stainless-steel plate (27.9 cm diameter) which is mounted in the target chamber. The position of all elements on the table is determined kinematically by precision-ground sapphire balls. The incident beam is aligned by centering it in the input and $(e, e')$ alignment apertures (see Fig. 2) with no target in the beam. The alignment apertures are 1.5 times the diameter of the beam at their location so that vignetting does not occur. A target is then placed in the beam and the alignment deflectors on the $(e, 2e)$ beam arms are adjusted for maximum elastic flux. This ensures that the cone of scattered electrons which is accepted by the pupil and window aperture has been centered in the alignment aperture on the $(e, 2e)$ beam line.

## III. ELECTRONICS

### A. dc voltage distribution

A fundamental feature of high-energy $(e, 2e)$ scattering is the necessity of having two of the three components— electron gun, target chamber, and detector—at a high potential. We chose to place the detectors near room ground to simplify coupling signal pulses to the electronics. The electron gun is at $-12.5$ kV and all input electron lens voltages float on this potential. The target is at $+12.5$ kV. The voltage supplies for the output lens and Wien filter all float on a variable voltage $V_b$ which has a range $0 < V_b < 80$ V. The $-12.5$- and 12.5-kV supplies are slaved together so that the

binding energy we observe, $E_b = E_s + E_r - E_0 = 2eV_b$, is independent of the incident beam energy. The variable voltage $V_b$ is supplied by a computer-programmed DAC. Zero binding energy is calibrated by grounding the electron gun and observing the elastic peak from the target.

The voltages across the deflectors in the target chamber which determine the scattering angles (and, therefore, the target electron momentum $q$) are provided by BERTAN supplies. An analog voltage of 0 to $-5$ V drives the BERTAN supplies full range. This voltage is controlled by computer. A serial 7-bit number from the computer is transmitted by an optoisolator UART link to an analog converter floating at the target chamber potential. An eighth bit from the computer controls a relay which determines the polarity of the voltage across the deflectors.

### B. Pulse electronics

Electrons with velocity in the bandpass of the energy analyzers are detected by a fast, linearly focused, discrete dynode electron multiplier (model D233, EMI Gencom). The glass envelope of the electron multiplier is attached through a glass-to-metal adaptor to a standard Conflat flange which attaches to the end of the beam arm vacuum jacket. The signal pulse from the electron multiplier goes to a preamp (EMI Gencom model VA.02) through a HV decoupling capacitor and then to a discriminator (Canaberra model 1428A). For $(e, 2e)$ measurements, the pulse from one of the two discriminators starts a TDC (time-to-digital converter, LeCroy model 2228A). A pulse from the other discriminator, delayed by approximately 13 ns, stops the time conversion. The time resolution of the TDC is 1/4 ns. The output of the TDC is read and stored by computer. The pulses from each discriminator also are counted by two scalers (Kinetics model 3640).

The acquisition of data is done by an LSI 11-based MINC (mobile instrumentation computer made by DEC). As shown in Fig. 6, the variable potential $V_b$ which determines the binding energy of the detected coincidence electrons is controlled by a DAC. The voltage supplies for the deflectors which vary the scattering angle are controlled through an optoisolator by a serial port of the computer. The TDC and scalers interface to the computer by standard CAMAC hardware. Data are stored initially on a floppy disk, then transferred at a convenient time to a file on the university mainframe computer for further analysis and plotting.

The primary consideration in developing the software for data acquisition is to minimize the systematic errors which arise from drift in the tuning of the spectrometer. This includes variation in the beam current and in the transmission efficiency through the electron optics. The systematic error can be largely eliminated by sweeping many times through all the binding energies and scattering angles of interest. The period for a single sweep is chosen to be less than the drift time of the spectrometer. Also, the parameter space (binding energy and scattering angle) is covered in random order each sweep. The absolute cross section cannot be determined by this procedure, but generally it is the relative cross section which is of primary interest. This data-acquisition technique is easily implemented by computer.
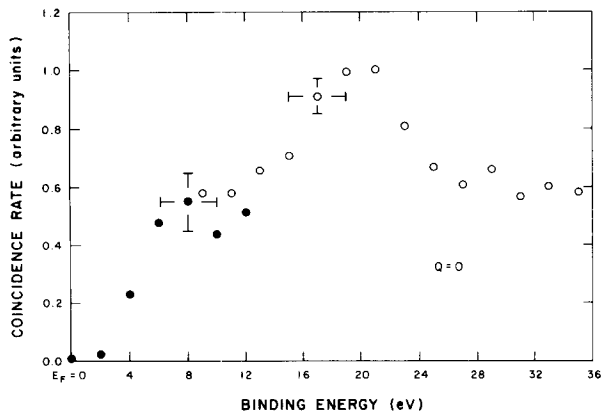
FIG. 7. Spectral momentum density (normalized to count rate at $E_b = 20$) of amorphous carbon as a function of $E_b$ for $Q = 0$. Open and closed circles are two different samples.



FIG. 8. Coincidence time spectra for $E_b = 20$ eV and $Q = 0$.

## IV. MAGNETIC SHIELDING

The target chamber, electron gun, zoom, and energy analyzers are surrounded by mu-metal shields. The shield for the target chamber is split in half for target access and provides insufficient shielding of the vertical magnetic field component. A Helmholtz coil concentric with the vertical axis of the target chamber is used to reduce the total field in the scattering chamber to $< 0.05$ G. Continuous mu-metal shielding cannot extend across the HV insulators in the beam lines. These sections were shielded with a series of mu-metal rings (30.5 cm o.d, 17.8 cm i.d, and 0.16 cm thick) which are 1.9 cm apart and are mounted on Plexiglas rods. These rings shield the vertical component of field on the beam axis by factors of 10 to 100. The parallel component is not shielded, but the effect of this component on the focusing of the beam can be compensated. The theory of this shielding technique is described by Gibbons et al.[12]

## V. RESULTS

We have observed coincidence spectra for $(e, 2e)$ scattering from an amorphous carbon film (from Arizona Carbon Foil). The preliminary data at $Q = 0$ as a function of binding energy are shown in Fig. 7. The energy resolution is 4 eV (FWHM) and the momentum resolution is 0.8 Å$^{-1}$ (FWHM). One set of data (open circles) are from an unsupported carbon film (placed across a 2.5-mm-diam hole) which is nominally 110 Å thick (film density $= 2.4 \mu g/cm^2$). This film broke after taking data for 1 month. We discovered the calibration of $E_b$ was incorrect for these data after the film broke; this is the reason the data extend to $E_b = 0$. The second set of data (closed circles) are from a supported carbon film (50 mesh copper grid) which is nominally 90 Å thick ($2.0 \mu g/cm^2$). The coincidence rate for the supported film is a factor of 4 less than the rate for the unsupported film. The coincidence spectra at $E_b = 20$ eV is shown in Fig. 8. The coincidence rate at this energy is 0.014 Hz. The width of the coincidence peak is 4 ns, which is approximately the same width as observed by others in gas $(e, 2e)$ experiments.

The position of the Fermi energy is determined by calibrating the pass energy of the Wien filter from the elastic
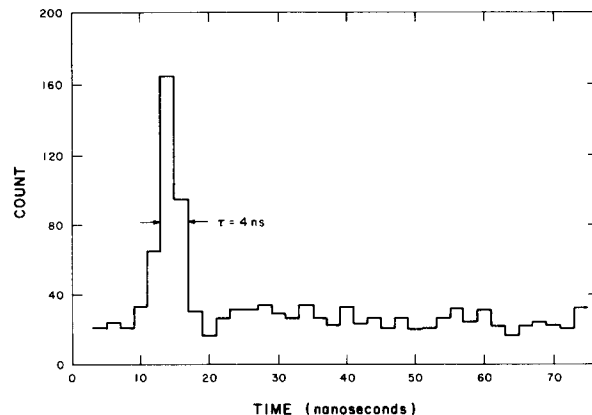
peak and by measuring with a Fluke precision high-voltage divider (Fluke 80F-15) the potential of the target and the electron gun cathode. If the target and the cathode are conductors, the binding energy of the target electron is

$$E_b (\text{with respect to } E_F) = e(VN - VP) - KE_T + 2e\Delta V_b ,$$

where $VN$ is the magnitude of the cathode potential, $VP$ is the magnitude of the target potential, $KE_T$ is the average thermal energy of electrons leaving the cathode, and $e\Delta V_b$ is the variable pass energy of the analyzer with respect to the elastic peak. We monitor the difference $VN - VP$ with two Fluke probes and find that it varies by less than 1 V. The variable voltage $\Delta V_b$ is controlled by a DAC in the computer. We estimate the uncertainty in $E_b$ is $\pm 1$ eV. If the amorphous carbon film is insulating, the uncertainty is larger due to charging. The sharp drop in the coincidence rate to zero at $E_F$ indicates that our calibration is correct.

The elastic scattering rate from the unsupported carbon film into one arm of our spectrometer is of order 2 MHz for an incident beam energy of 12.5 keV. We did not measure it accurately because the electron multiplier was saturating at this high rate. The elastic rate in the other beam arm is $\sim 700$ kHz. The rates should be equal, of course, if the transmission efficiencies of both arms are the same. The lower rate in one arm is apparently due to a mechanical misalignment which we are correcting. The theoretical rate for scattering electrons from the carbon nucleus (the electronic form factor is negligible at our momentum transfer of $\sim 60$ Å$^{-1}$) is 7 MHz for the parameters of this measurement. Approximately two-thirds of this theoretical figure is lost due to multiple scattering. We observe a broad spectrum ($\sim 30$ eV wide) centered approximately 25 eV below the elastic peaks. These electrons undoubtedly suffer a small angle inelastic collision before or after scattering elastically by $\sim 45°$. The total integrated count under this broad peak is approximately twice the count in the elastic peak. After correcting for this loss, the difference between the observed and theoretical elastic rate suggests that the transmission efficiency of our "good" beam arm is quite high. It should be noted that the multiple scattering contribution to the $(e, 2e)$ spectra will not be as high as we observe in the elastic measurement because the incident energy is 25 keV for the coincidence measurements.

The inelastic electron–electron scattering rate from the unsupported carbon film was $\sim 800$ Hz in the good beam

arm and 200 Hz in the other beam arm. This rate was measured with an incident beam energy of 25 keV and a beam current which was approximately two or three times larger than the incident current for the elastic measurement. We estimate that the ratio of the elastic and inelastic count rate under the conditions of our measurement is roughly 6000, in reasonable agreement with the measured ratio.

The $Q = 0$ spectra have a conspicuous peak at 20 eV and a sharp shoulder at 8 eV. There is a broad hump beginning, apparently, at this shoulder and extending beyond 48 eV (limit of our present measurements). We tentatively ascribe this background to multiple scattering. We expect it to be relatively smooth and featureless for amorphous carbon, but this conjecture will be checked by a more detailed analysis. The density of states for amorphous carbon also peaks at $\sim 20$ eV as seen in photoemission spectra.[13] Since our energy and momentum resolution are relatively low, it is not surprising that the data are similar. There is considerable interest in determining whether the bonds in amorphous carbon are graphitic or diamond in character. Most evidence suggests that the bonding is primarily threefold in nature with some fourfold diamond bonding.[14] The structure of amorphous carbon varies considerably depending on the preparation details. The peak we observe at 20 eV might be associated with the lowest band in graphite which is also at the same energy. The shoulder at 8 eV possibly arises from the upper three bands in graphite, but it is difficult to understand why the peak at 20 eV is much stronger than the structure at 8 eV. We see no structure at 30 eV which might be identified with the lowest diamond band. We are presently taking data at different values of $Q$ to shed further light on this question.

Clearly $(e, 2e)$ spectroscopy has considerable potential for elucidating the electronic structure of amorphous and crystalline materials. The low count rate is the major impediment to full utilization of the technique at this time, and would be an even more serious problem if the energy and momentum resolution were improved or if the incident ener-

gy were increased. But there appears to be no technical reason that data at different binding energies and momenta could not be taken simultaneously in parallel, rather than in serial, order. We estimate that to double the incident energy, the energy resolution and the momentum resolution simultaneously will require $\sim 64$ data collection channels to maintain the present data rate. It is not inconceivable to have several hundred data channels.

## ACKNOWLEDGMENTS

[1]U. Amaldi, Jr., A. Egidi, R. Marconero, and G. Pizzella, Rev. Sci. Instrum. **40**, 1001 (1969).
[2]R. Camilloni, A. Giardini Guidoni, R. Tiribelli, and G. Stefani, Phys. Rev. Lett. **29**, 618 (1972).
[3]E. Weigold and I. E. McCarthy, Adv. At. Mol. Phys. **41**, 127 (1978).
[4]I. E. McCarthy and E. Weigold, Phys. Rep. C **27**, 275 (1976).
[5]B. Lohman and E. Weigold, Phys. Lett. A **86**, 139 (1981).
[6]I. E. McCarthy, A. Ugbabe, E. Weigold, and P. J. O. Teubner, Phys. Rev. Lett. **33**, 459 (1974).
[7]R. Camilloni, A. Giardini Guidoni, I. E. McCarthy, and G. Stefani, Phys. Rev. A **17**, 1634 (1978).
[8]G. Stefani, R. Camilloni, and A. Giardini Guidoni, Phys. Lett. A **64**, 364 (1978).
[9]J. H. Moore, M. A. Coplan, T. L. Skillman, Jr., and E. D. Brooks, III, Rev. Sci. Instrum. **49**, 463 (1978).
[10]C. E. Kuyatt (unpublished).
[11]W. H. J. Andersen, Br. J. Appl. Phys. **18**, 1573 (1967).
[12]P. C. Gibbons, J. J. Ritsko, and S. E. Schnatterly, Rev. Sci. Instrum. **46**, 1546 (1975).
[13]F. R. McFreely, S. P. Kowalczyk, R. G. Cavell, R. A. Pollak, and D. A. Shirley, Phys. Rev. B **9**, 5268 (1974).
[14]J. Robertson, Adv. Phys. **32**, 361 (1983).